CERN – EUROPEAN ORGANIZATION FOR NUCLEAR RESEARCH

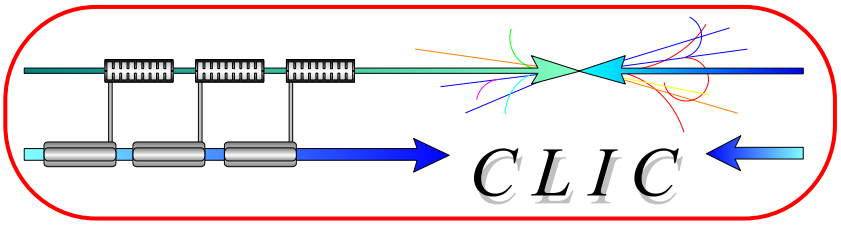

CLIC Note 548
PS/AE Note 2002-199

LASER WIRE SIMULATIONS FOR THE CLIC BEAM DELIVERY SYSTEM USING GEANT4

Gregory Penn

CERN-OPEN-2003-003
08/01/2003

Abstract

The laser wire scanner (LWS) is a non-destructive beam diagnostic which has been proposed for CLIC and other very low emittance electron beams. Measurements of the beam size can be made with submicron resolution. Different configurations for detecting scattered electrons are simulated using GEANT4, and the signals compared with the backgrounds resulting from expected halo losses. The requirements of the LWS are compared with conditions in the CLIC Beam Delivery System. Measurements of emittance with better than 10% accuracy seem achievable for realistic parameters.

Geneva, Switzerland
8 January 2003

Laser Wire Simulations for the CLIC Beam Delivery System Using Geant4

G. Penn§, CERN, Geneva, Switzerland
UC Berkeley Dept. of Physics, Berkeley, CA 94720

Abstract. The laser wire scanner (LWS) is a non-destructive beam diagnostic which has been proposed for CLIC and other very low emittance electron beams. Measurements of the beam size can be made with submicron resolution. Different configurations for detecting scattered electrons are simulated using GEANT4, and the signals compared with the backgrounds resulting from expected halo losses. The requirements of the LWS are compared with conditions in the CLIC Beam Delivery System. Measurements of emittance with better than 10% accuracy seem achievable for realistic parameters.

1. Introduction

The laser wire scanner (LWS) has been proposed as a diagnostic in CLIC and other very low emittance electron beams. Diagnostics to measure the beam are needed to commission the lattice, to optimize performance, and for physics experiments. The LWS is rapid, non-destructive (small total cross section), and can be used to measure the relative number of electrons intersecting the laser beam. If the laser width is sufficiently small, this allows for a transverse density scan, but does not directly measure beam angles. LWS promises submicron resolution and, unlike true wires, all of the hardware is well separated from the beam and so protected from damage. There are, however, concerns about how to detect the scattered electrons or photons, and about background levels. Because of the collimation and much larger beta functions in parts of the Beam Delivery System (BDS), the requirements for the LWS are examined in terms of BDS parameters to determine what, if any, constraints a laser wire scanner would impose on the BDS.

2. Compton scattering

The Compton scattering process can be analyzed most simply by examining the physics in the rest frame of the electrons. We consider a laser with frequency ν intersecting an electron beam with energy $E_B = m_e c^2 \gamma_B$. In the electron rest frame, the photon is upshifted by γ_B (or $2\gamma_B$ if originally antiparallel), to the frequency $\nu' \simeq \gamma_B \nu$.

§ gpenn@socrates.berkeley.edu

The scattering process in the electron frame depends on the Compton parameter [1] $\xi = h\nu'/m_e c^2$. In the Thomson regime, $\xi \ll 1$, the photon energy is still less than the electron rest mass, and the collision will be nearly elastic. Photons which are backscattered then get upshifted by another factor of $2\gamma_B$ in the lab frame. Thus, scattered photons have frequencies as high as $2\gamma_B^2\nu$ with angles $< 1/\gamma_B$. The electrons, however, are only slightly affected by the interaction. In the Compton regime, $\xi \gtrsim 1$, the photon can acquire most of the electron's energy, although the final electron energy is at least $m_e^2c^4/2h\nu$, so that the final $\gamma > \gamma_B/2\xi$. The typical angle for scattered photons, which is also the maximum angle of electrons, is $\sim \xi/\gamma_B \simeq h\nu/m_e c^2$. Electrons at the largest scattering angle have energy $\sim \gamma_B m_e c^2/\xi$.

The main demands for LWS are to have a large signal and good resolution. The spread of the laser beam can be subtracted from the measured size of the beam, but the effectiveness of this is limited by how well the laser is characterized, and the shape of the electron beam modifies the correction as well. The total number of scattering events depends on the electron beam only through its spatial distribution and energy. The rms dimensions of the electron beam are given as σ_x, σ_y, and σ_z, while the laser pulse will be defined by its wavelength $\lambda = c/\nu$, duration τ_L, peak power P_L, and minimum spot size σ_{L0}. The spot size σ_{L0} is the rms in intensity of the laser at its focus, which is half of the "waist" in laser terminology. Considering a measurement of the profile in y, the conditions for accurate measurement of the electron beam are $\lambda < \sigma_{L0} < \sigma_y$, and $\sigma_y/\sigma_x > M^2\lambda/2\pi\sigma_{L0} =$ angle of laser cone. The quantity M^2 is the ratio of the Rayleigh length of an ideal, single-mode Gaussian beam to the actual Rayleigh length due to the presence of higher order modes. Thus the constraint on the laser wavelength in order to be able to measure a given beam is

$$\lambda \ll \frac{\sigma_y^2}{\sigma_x}\frac{2\pi}{M^2}. \tag{1}$$

For a given wavelength, the shape of the electron beam and the M^2 of the laser strongly affect the minimum beam size that can be measured.

If the laser satisfies

$$c\tau_L \gg \sigma_{L0},\ \sigma_x, \tag{2}$$

the number of scattering events scales as

$$N_{\rm scat} \propto N_e P_L \frac{\lambda}{\sigma_y}\frac{c\tau_L}{(c^2\tau_L^2+\sigma_Z^2)^{1/2}}\frac{\lambda}{E_B}, \tag{3}$$

where N_e is the total number of electrons in the bunch. The last factor only applies in the Compton scattering regime. To maximize the signal, it is preferable to take as large λ and τ_L as is consistent with the desired resolution. To detect degraded electrons, it is also necessary to be in the Compton regime with large $\xi = h\nu'/m_e c^2 \simeq 5E_B[\mathrm{TeV}]/\lambda[\mu\mathrm{m}]$. Then for higher energies, more laser power will be needed to obtain the same signal.

3. Modelling of laser wire scanner

The scattering of electrons by the laser beam is easily simulated, and the resulting particles have been tracked in several simplified detector and magnetic field geometries. In addition, more sophisticated GEANT4 [2] simulations have been used to model interactions with materials and the detection process itself. The following have been taken as parameters for the CLIC beam at the intersection with the laser: 0.67 nC charge per bunch, $E_B = 1.5$ TeV, $\epsilon_x = 680$ nm, $\epsilon_y = 10$ nm, where ϵ is the normalized emittance. In the CLIC BDS, where beam sizes are of the order of 10 microns, typical angles are only 10 nrad; because the derivatives of the beta functions can be extremely large, the correlated beam angles can be as large as the uncorrelated values. Even so, these angles are so small as to be completely negligible, as is the energy spread of order 160 MeV. Thus, for such small emittances, the signal from the LWS is sensitive only to the physical size of the beam.

For the laser, we will consider mainly 400 nm wavelength light, although smaller wavelengths may be desirable for extremely small beams. The pulse duration of 0.12 ps matches the 35 μm bunch length. The scattering parameters are $h\nu/m_e c^2 \simeq 10^{-5}$, and $\xi \simeq 30$. The laser wavelength will turn out to be a crucial factor in the analysis, so in order to maintain a consistent level of realism we consider a laser producing 2 mJ pulses at 800nm wavelength. These pulses can then be doubled or tripled in frequency, at significant cost to the available laser power. It is assumed that 1 mJ of energy remains after conversion to 400 nm wavelength, and that a frequency tripler yields 0.5 mJ of energy at 267 nm. The M^2 of the laser is important mostly for the limitations in the size of the electron beam that can be measured, according to Eq. (1). Thus, if tripling the laser frequency results in a dramatic decrease in laser quality and increase in M^2, there may be no improvement in resolution. Here, we assume $M^2 = 3$ throughout.

We examine a baseline case of a round, 10 μm beam, scanned using 400 nm laser light at 1 mJ per pulse. Under these conditions, and with a laser waist (twice the minimum σ_y) of 4 μm, there are roughly 14000 scattering events per pulse. For the diagnostics, we consider placing a 1 m long detector next to the beam pipe; the degraded electrons, after hitting the beam pipe, will produce secondaries which deposit energy in the detector. A simple dipole field, set to 100 gauss, seems to be the best method for sweeping out the degraded electrons. Long dipole fields of 50 and 100 gauss already occur in the BDS design.

For a beam energy of 1.5 TeV, intersecting a 1 mJ pulse of 400 nm laser light, the distribution of scattered electrons and photons are shown in Figures 1 – 3. There is a large population of electrons in the range 50 – 150 GeV, with corresponding photons that acquire the bulk of the original electron energy. This also corresponds to a peak in scattered angle of the electrons at 6 μradian. The photon distribution peaks at angles of approximately 0.5 μradian. Using sextupoles to select the degraded electrons based on scattering angle has been looked at previously [3], and found to be less satisfactory than using a long dipole field to select particles based on energy.

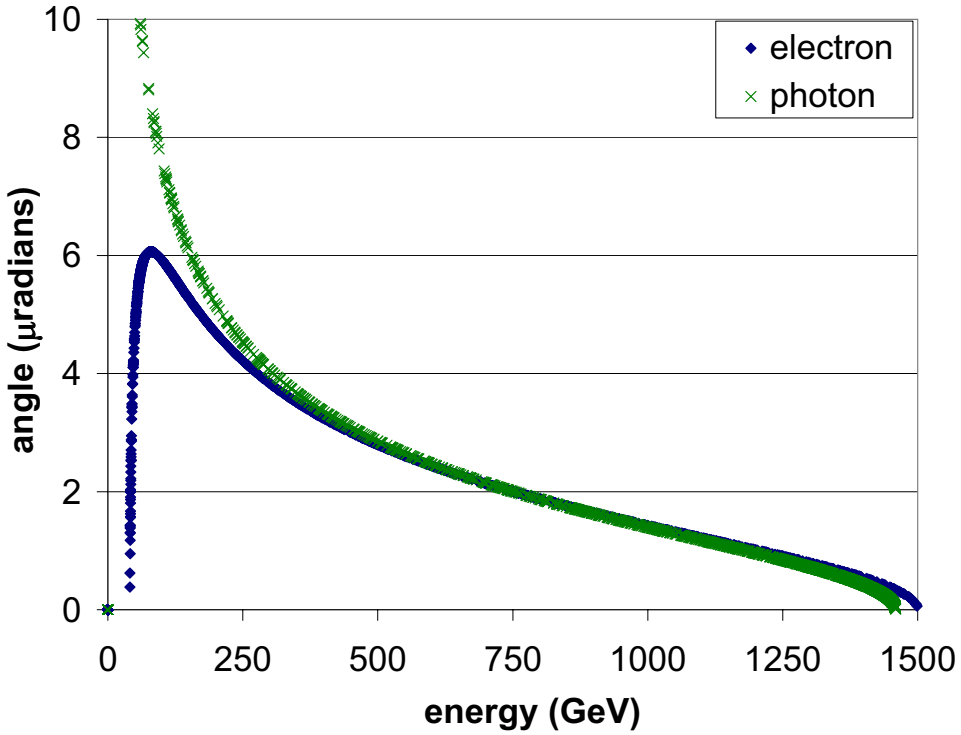

Figure 1. Distribution of scattered electrons and photons.

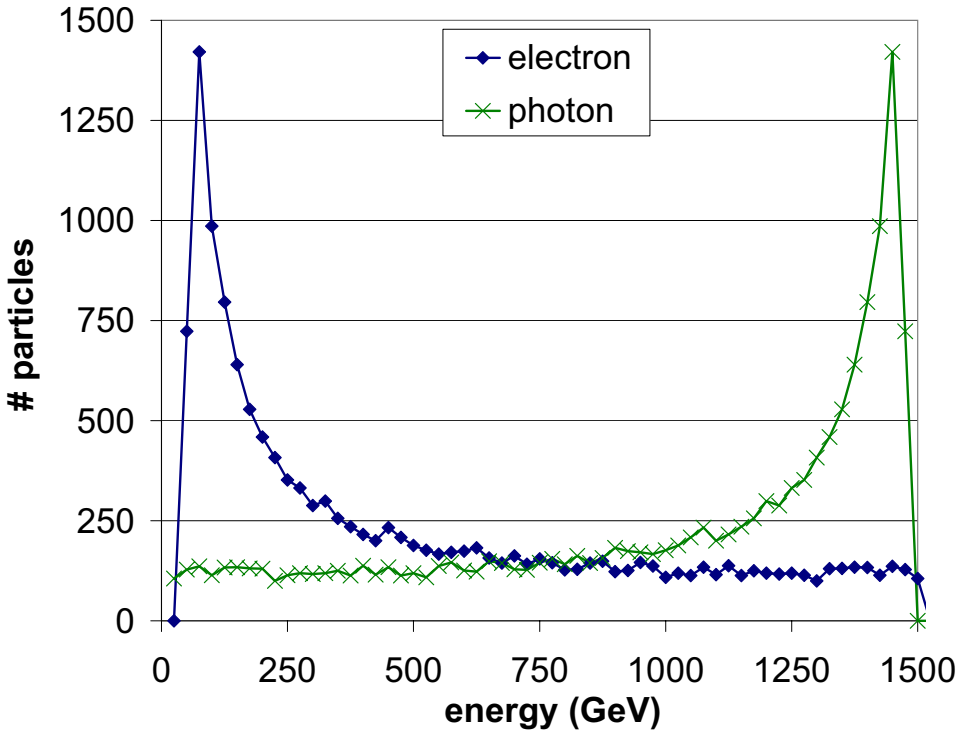

Figure 2. Histogram of scattered electrons and photons by energy, in 25 GeV bins.

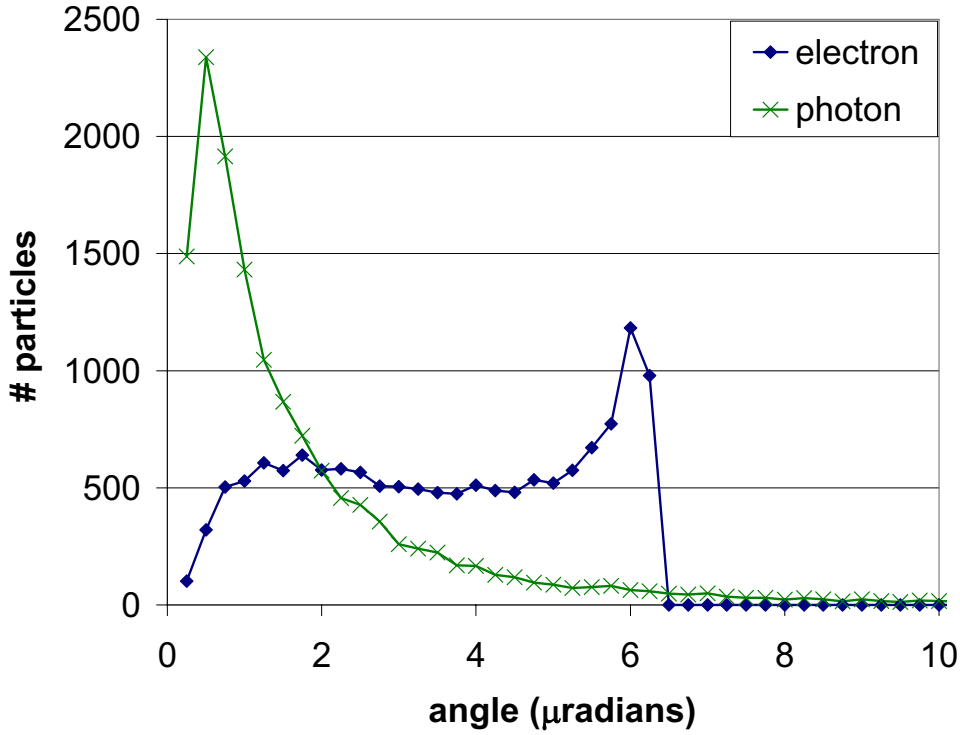

Figure 3. Histogram of scattered electrons and photons by angle, in 1/4 μradian bins.

4. GEANT4 Simulations

The detection of degraded electrons produced by a laser wire scanner has been studied using GEANT4. A dipole field was used to sweep out the low energy electrons from the beamline. The dipole field was assumed to ramp up from zero to a typical value of 100 gauss immediately after the intersection of the beam with the laser wire. The beampipe is taken to be straight until this intersection, then curved with the appropriate radius of curvature. However, in the current version of GEANT4 (v4.4.1), toroidal shapes do not seem to work properly; instead, this geometry was approximated using a series of cylinders centered at points which lie along a circular arc, and almost touching at their inner bends. This produces very small gaps in the pipe, but the gaps should not affect the results. Hopefully, this issue will be resolved in future revisions of the code.

The beampipe has been uniformly taken to have a 1 cm radius, and to be 1 mm thick. Thicker beampipes do reduce the signal, but not by a disproportionate amount. The detector is a cylinder of Argon gas, with 1 m length and 2 cm radius, holding approximately a liter. The dipole magnet was modelled as two very long iron blocks, 20 cm wide and 10 cm thick, separated by 5 cm. Thus, there is a gap of 1.4 cm between the beampipe and each side of the magnet. In addition, different arrangements of iron blocks to shield the detector were considered.

5. Simulation Results

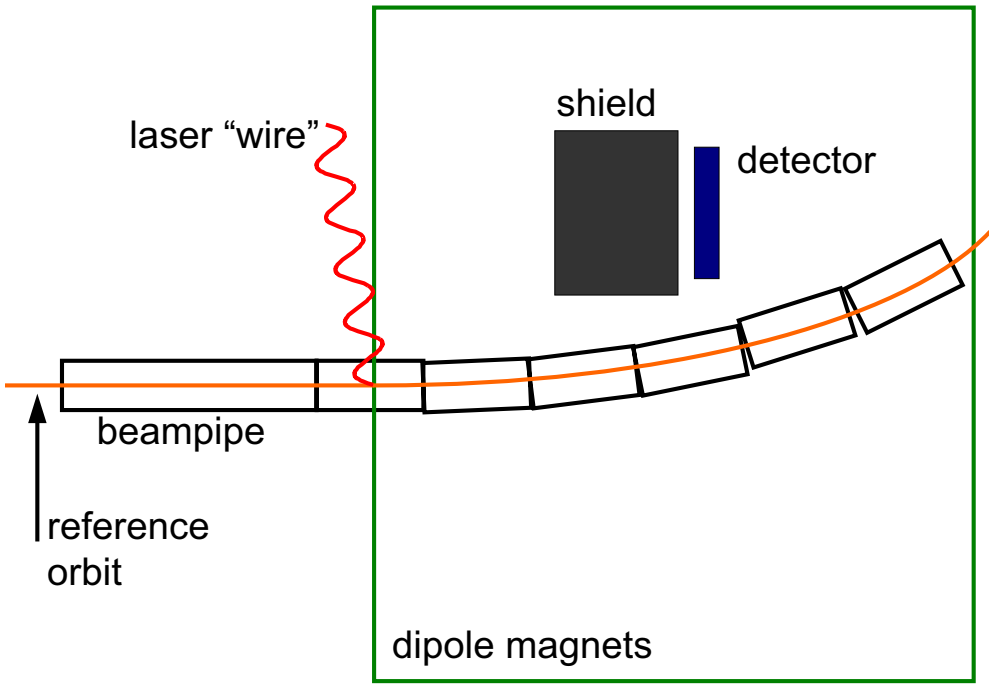

Figure 4. Diagram of the geometry for the detection of degraded electrons. The horizontal scale is very exaggerated.

The best case considered so far is a 1 m long detector in a dipole field with a single shield in front of the detector. The configuration is illustrated in Figure 4. Typically, the detector was composed of Argon gas at standard density. The detector and shield were both positioned so as to be separated from the beampipe by 1 cm. At this location, the material in the detector does not significantly affect the results. Previous results, when the the detector was placed closer to the beampipe, showed reduced signal to noise ratios when denser materials were used in the detector. The shield was positioned so as to have a 1 m gap between it and the detector. This configuration is not fully optimized, but moderate changes in the geometry do not seem to produce large changes in the results. In Figure 5, the extraction of the degraded electrons is examined as a function of the distance of the center of the detector from the laser wire. In addition to the total energy deposited in the detector (left hand scale), we note the number of electrons which produce “significant” hits (right hand scale), defined as having an energy deposition above half of the average value deposited into the detector. With this measure, the efficiency of the detector is roughly 5%, which is low but still reasonable. This is used as an indication of the statistical fluctuations of the signal due to the small total number of measured events. The consequences of such low statistics will be examined more closely below. Note that because the dipole field bends the main beam as well, the possibility also exists of detecting the photons. The energetic photons

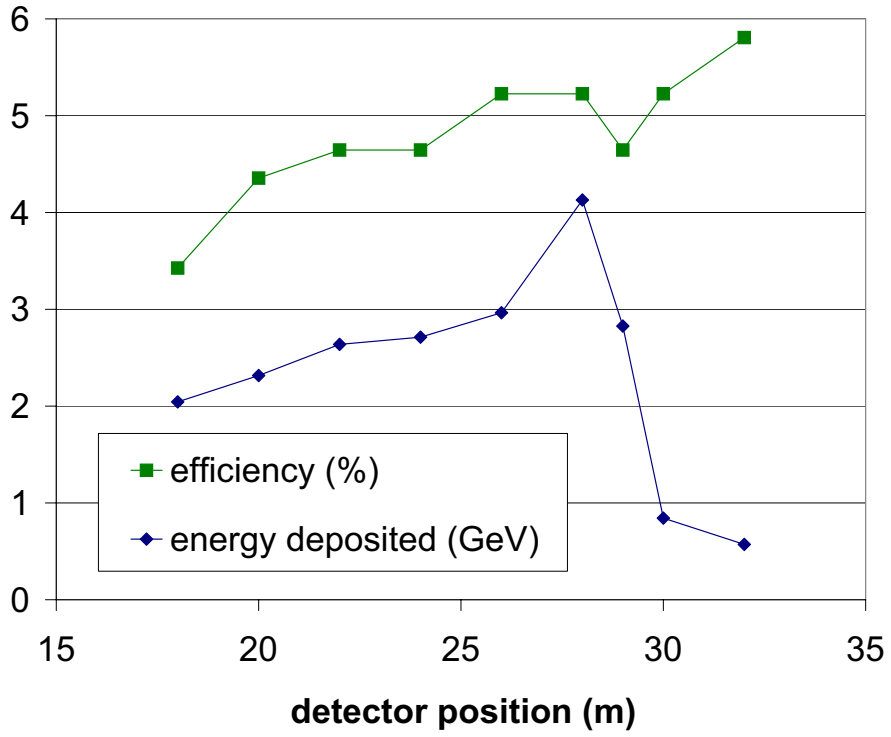

Figure 5. Variation in the energy deposited in detector as a function of distance from laser wire, for a uniform dipole field of 100 gauss and a 400 nm laser.

will occupy a very narrow cone in angle, but detection of TeV-range photons may be a complicated problem.

For the degraded electrons, the results are as follows: using a 400 nm laser with a 10 micron spot size, the optimum signal in the simulations occurs when the detector is placed 28 m upstream of the laser wire, and with the laser wire aligned to maximize the signal. With this geometry, about 3.3 GeV is deposited in the detector, with a significant contribution from 770 particles, using a cutoff of 0.65 MeV. The maximum energy deposited per degraded electron is 12 MeV. Using a 267 nm laser with a 2 micron spot size, the optimum occurs for a detector placed 20 m upstream of the laser wire. With this geometry, about 2.7 GeV is deposted in the detector, with a significant contribution from 1000 particles, using a cutoff of 0.53 MeV. The maximum energy deposited per degraded electron is 7 MeV.

The laser parameters are compared against commercially available lasers in Table 1. The "effective energy" is defined to be the equivalent energy of a laser overlapping a single bunch, as in the design parameters, necessary to yield the same rate of scattering events. Thus, the effectiveness of the Nd:YAG laser is enhanced by the fact that it overlaps multiple bunches, but reduced by the low repetition rate. For the Nd:YAG laser, the low effective energy does not indicate any difficulty in achieving a signal comparable to that found for the design parameters, only that measurements will take longer to complete by a factor of 10. Also, note that the Ti:Sapphire laser is only off

Table 1. Laser parameters compared with commercially available lasers.

	Design	Nd:YAG	Ti:Sapphire
wavelength	800 nm	1064 nm	800 nm
pulse FWHM	150 fs	3 ns	50 fs
energy per pulse	2 mJ	2200 mJ	0.7 mJ
rep rate	100 Hz	10 Hz	1 kHz
energy fluct	-	8%	1%
peak power:			
at 532 nm	-	0.35 GW	-
at 400 nm	5 GW	-	5 GW
at 267 nm	2.5 GW	0.05 GW	2.5 GW
effective energy (at 400-532 nm)	1 mJ	0.1 mJ	0.5 mJ

by a factor of 3 in energy per pulse, with a repetition rate ten times what is needed. It is possible that such a laser could be adapted to provide the desired power at 100 Hz. The efficiency for converting 800 nm laser light to a 267 nm wavelength may in practice be worse than the assumed value of 25%; the corresponding efficiency for converting 1064 nm light to 267 nm seems to be less than 10%. For short laser pulses, proper synchronization between the laser and the electron bunch may also be an issue. In summary, we see that current laser technology approaches the desired performance for a laser wire scanner, but either future improvements in commercial technology or custom-designed lasers may be needed for a practical device.

For comparison, laser wire scanner experiments from CTFII operated in the Thomson regime by using a 2.5 mJ laser at 1 micron wavelength to measure a 50 MeV electron beam [4]. In this case, the upshifted laser light is detected; for the experimental geometry used, about 600 photons were expected to hit the detector with each laser pulse. At the lowest noise levels experienced in the beam, the ratio of expected signal to the measured backgrounds was approximately 1:8. Even with these low statistics and large level of noise, by averaging over several scans the backgrounds could be subtracted out sufficiently to observe the profile of the electron beam. Although consistent with the known beam profile, the resolution was still too low for an accurate measurement. Below, we will examine more quantitatively the expected backgrounds and the dependence of the achievable accuracy of the profile measurement on signal and background levels.

6. Estimate of backgrounds and signal to noise ratio

To analyze the usefulness of these schemes, it is necessary to also consider the backgrounds introduced by beam losses, which occur throughout the beam line. The beam losses produce a large spray of secondaries which will also deposit energy in the detector. The backgrounds are estimated to be the result of a loss of halo electrons

hitting the beam pipe at a rate of one per meter per bunch. This very low loss rate probably limits the LWS to be used after some sort of beam collimation. The BDS, one of whose essential functions is beam collimation, is thus a reasonable place to attempt to situate the laser wire system. In addition to the schemes analyzed here, it may also be possible to detect the scattered, upshifted photons. There, the signal must be separated from halo losses and from synchrotron radiation.

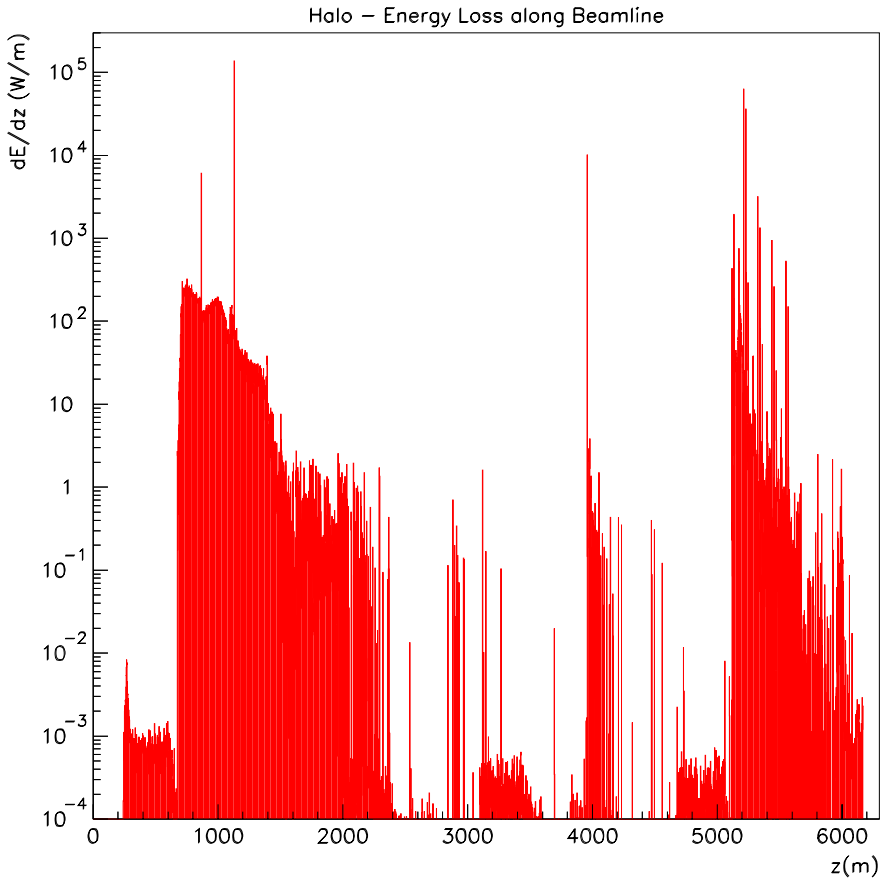

Figure 6. Simulated beam halo losses in the CLIC beam delivery system, in terms of power deposited per meter. From G. Blair, Ref. [5].

Simulations in GEANT4 allow for issues of detection and backgrounds to be addressed in a realistic way. The results are here presented in Table 2 in terms of energy deposited in the detector, for the degraded electrons and as well for the halo particles, assuming a nominal loss rate of 1 per meter. This corresponds to a time average of 3.7 mW per meter for the CLIC bunch structure. The results for a calculation of beam losses performed by G. Blair [5], given a 10^{-3} beam halo fraction, is illustrated in Figure 6. Several regions are apparent which fall below the 4 mW level of power deposition. An iron shielding block placed in front of the detector is seen to improve the ratio of signal to background. Without the shielding in front of the detector, halo losses from far

Table 2. Signal and background calculations in GEANT4. Design case is using 400 nm laser, with 100 gauss dipole field, gas detector, and a single shield. Given in GeV deposited in detector.

Parameters	Signal	Background (x4)
design	3.3	0.4
267 nm laser	2.7	0.4
unshielded	3.3	0.6
front and back shields	3.2	0.5
solid detector	4800	600
50 gauss	2.0	0.4
500 GeV beam	7.0	0.2

upstream can lead to hits in the detector. A similar shield placed behind the detector, however, provided no benefit.

Because the detector response time will probably be longer than the time between electron bunches, the signal from the LWS will have to compete against halo losses from multiple bunches in the train; assuming a detector response time of 3 ns, this implies an enhancement in background by a factor of 4 but no corresponding enhancement in the signal. Taking this into account, simulations show that for a 1 m long detector, with a single long shield 1 m upstream, about 400 MeV is deposited in the detector from halo losses. There are 120 particles which are above the cutoff, defined as half the average energy deposited, or in this case 1.1 MeV. The maximum energy deposited by a single halo particle was 18 MeV.

For the 400 nm laser configuration, the signal to noise ratio is 8:1. Because the signal is proportional to $1/\sigma_y$, the ratio improves for smaller beam sizes. The limiting beam size is roughly $\sigma_y > 2$ μm, although if the horizontal size is kept at 10 microns, then the vertical size cannot be reduced below about 4 μm. Of course, the laser waist will have to be reduced along with the beam size. Improving M^2 would allow for even smaller beams to be measured, with correspondingly higher signals. Similarly, for a 267 nm laser, the minimum spot size would be roughly 1 μm assuming that the beam was close to round; otherwise even 267 nm laser light will not work unless the laser M^2 can be made close to unity.

If the size of the electron beam could vary from as low as 1 micron to greater than 10 microns, then it will be necessary to have the option of choosing among several laser frequencies, which in this case means switching between different frequency multipliers. For even larger beam sizes, an 800 nm wavelength would be preferable. This can be accomplished without too much difficulty either by having two detectors, or by placing the detector in a compromise position, say 25 m downstream from the intersection of the laser with the electron beam.

Table 3. Reconstructions of beam size.

Ratio of background to peak signal	Fluctuations in: peak signal	fitted peak	σ_y	σ_y due to background
0	2.2%	0.9%	2%	-
0.1	2.5%	1%	2.6%	1.7%
0.25	3.0%	1.6%	4.1%	3.6%

7. Reconstruction of beam size and emittance

Because of the finite spot size of the laser, the LWS will not directly yield the true profile of the beam, but will depend on the laser properties as well. Diffraction of the laser beam will also affect the measured beam size. Under the assumptions of Eq. (2), together with the condition that

$$\sigma_R \equiv \frac{\lambda M^2 \sigma_x}{2\pi\sigma_{L0}} \ll \sigma_y, \tag{4}$$

we can approximate the contributions to the measured beam radius as

$$\sigma^2_{\rm meas} \simeq \sigma^2_y + \sigma^2_{L0} + \sigma^2_R. \tag{5}$$

The quantity σ_R represents the additional effective size of the laser beam due to its diffraction, if the Rayleigh range of the laser is comparable to the horizontal size of the beam. Fluctuations due to background and to low statistics will further complicate the calculation of the beam size. The laser profile correction can easily be kept below 10%, and the laser waist can be measured accurately. The term due to diffraction of the laser beam is more difficult to determine with a high accuracy, and should be kept below a few percent. These conditions essentially determine the maximum wavelength light which can be used for a high accuracy measurement, and are equivalent to the conditions given in Section 2.

It is possible to observe these constraints in the CLIC BDS, and so we assume that systematic effects such as the contribution from σ_{L0}, etc., can be accurately subtracted out. The process of reconstructing σ_y is then examined under the following assumptions: the peak signal, when the laser is centered, consists of 2000 detected particles; the fluctuations in the signal are purely statistical; and background fluctuations are 10% of the average, which is larger than the purely statistical level. The laser wire scan consists of 10 measurements taken across the beam; thus, a single scan of the beam profile would take 0.1 s. The "measured" beam size was then calculated using a basic parametric fit to a Gaussian, allowing for displacements and a constant background. The results are shown in Table 3.

More generally, we find the following:

- In the absence of backgrounds, the error in σ_y is roughly the inverse square root of the peak number of particles detected. The statistical fluctuations in the tails are

worse than this, but there may in fact be a better algorithm for reconstructing σ_y.

- Backgrounds introduce additional errors, on the order of 1.5 $\times$ (background fluctuations) / (peak signal). This error adds in quadrature to the statistical error from the signal itself.
- The reconstructed peak line density has half the statistical error of the width σ_y when there are no backgrounds. With backgrounds, this difference is even more pronounced.
- The emittance is equal to σ_y^2/β_y; the fluctuations in measuring σ_y^2 can be kept below 5% for a signal to noise ratio ≥ 10. In fact, at this level the statistical noise in the signal itself is the most significant problem.

Because of this last point, any method which acquires more statistics can improve performance, even if the backgrounds are enhanced as well, so long as the signal to noise ratio of 10:1 can be achieved. Thus, although current simulations using the design parameters have yielded around 700 hits in the detector per scan, this can be scaled up by measuring 100 bunches per scan instead of 10. The penalty for this is that each emittance measurement would take 1 second.

Because the beam may not be exactly matched, a full emittance diagnostic would need to consist of a combination of measurements at different beam phases, which would then be combined into an emittance measurement. Because the LWS is non-destructive, these measurements can be performed simultaneously. In general, σ_y^2 must be measured at three locations, but for a small mismatch it is expected that the combined error will be less than twice that of the individual measurements. This implies that, so long as three suitable locations can be found, an accuracy of 10% in the beam emittance should be possible, although each scan may require 1 second to complete.

Measuring the beam size σ at three positions, labelled A, B, and C, the emittance can be reconstructed if the transfer maps between the three points are known. It is sufficient to know the values of the Courant-Snyder parameters for a beam having some target values at one of the points (a "matched" beam), as well as the phase advance between the points. If the transfer map between points A and B is written as

$$M_{AB} = \begin{pmatrix} r_{AB} & s_{AB} \\ t_{AB} & u_{AB} \end{pmatrix}, \tag{6}$$

it turns out that the emittance calculation from the beam sizes only depends on the three off-diagonal elements s_{AB}, s_{BC}, and s_{AC}. In terms of Courant-Snyder parameters, $s_{AC} = \sqrt{\beta_A \beta_C}\sin\Psi_{AC}$, where Ψ_{AC} is the phase advance between points A and C. The emittance can then be expressed as

$$\begin{aligned}\left(\frac{mc\epsilon}{P_z}\right)^2 = {} & \frac{\sigma_A^2\sigma_C^2}{2\beta_A\beta_C\sin^2\Psi_{AC}} + \frac{\sigma_A^2\sigma_B^2}{2\beta_A\beta_B\sin^2\Psi_{AB}} + \frac{\sigma_B^2\sigma_C^2}{2\beta_B\beta_C\sin^2\Psi_{BC}} \\ & - \frac{1}{4\sin^2\Psi_{AC}\sin^2\Psi_{AB}\sin^2\Psi_{BC}} \\ & \times \left(\frac{\sigma_A^4\sin^4\Psi_{BC}}{\beta_A^2} + \frac{\sigma_B^4\sin^4\Psi_{AC}}{\beta_B^2} + \frac{\sigma_C^4\sin^4\Psi_{AB}}{\beta_C^2}\right).\end{aligned} \tag{7}$$

This can be rewritten in a way that is less clearly symmetric, but is useful when considering error estimates:

$$\left(\frac{mc\epsilon}{P_z}\right)^2 = \frac{\sigma_A^2\sigma_C^2}{\beta_A\beta_C\sin^2\Psi_{AC}} - \frac{1}{4\sin^2\Psi_{AC}\sin^2\Psi_{AB}\sin^2\Psi_{BC}} \times\left(\frac{\sigma_B^2\sin^2\Psi_{AC}}{\beta_B} - \frac{\sigma_A^2\sin^2\Psi_{BC}}{\beta_A} - \frac{\sigma_C^2\sin^2\Psi_{AB}}{\beta_C}\right)^2. \tag{8}$$

The measurement at B can be thought of as correcting for certain types of mismatch of the actual electron beam. When $\Psi_{AC} = \pi/2$, then for a matched beam the second term vanishes. For small mismatches, the contribution of the second term, which is a small quantity squared, will be correspondingly small and should not contribute much to the overall error in the calculation. For general phase advance, the dominant error in the emittance calculation can be approximated as

$$\delta_\epsilon \simeq \sqrt{2}\,\delta_\sigma\left(\frac{1}{\sin^2\Psi_{AC}} + \frac{\cos\Psi_{AC}}{\sin\Psi_{AB}\sin\Psi_{BC}}\right) \tag{9}$$

where δ_σ is the relative error in the calculations of σ_y. Because the beam size must be obtained from the laser wire scan using Eq. (5), δ_σ will satisfy

$$\delta_\sigma^2 \simeq \delta_{\rm meas}^2\left(1 + \frac{\sigma_{L0}^2+\sigma_R^2}{\sigma_y^2}\right)^2 + \delta_{L0}^2\frac{\sigma_{L0}^4}{\sigma_y^4} + \delta_R^2\frac{\sigma_R^4}{\sigma_y^4}. \tag{10}$$

Here, $\delta_{\rm meas}$ is the relative accuracy in the numerical fit, which by the results above has the form

$$\delta_{\rm meas}^2 \simeq \frac{1}{\#\text{ of detected events}} + \left(\frac{0.15}{\text{ratio of signal to background}}\right)^2. \tag{11}$$

8. Conclusions

More simulations and optimization must be done to properly assess the requirements of a laser wire scanner for the CLIC beam. The possibility of detecting photons should also be explored further. Conditions in the BDS seem favourable for the inclusion of this diagnostic, although it is unclear whether a pair of such locations separated by $\pi/2$ will be readily available. At least two locations are necessary for measuring the emittance, and a third location is desirable to be able to account for a large beam mismatch. The size of the beam in the BDS is sufficient for the measurements; in fact, the total LWS cross-section becomes larger for smaller electron beams.

For full flexibility, to be able to measure the beam over a range of emittances and conditions, the LWS should probably be designed to operate over a range of frequencies. Even at 1 μm wavelength, the required resolution may be achievable for beams which are of order 10 microns wide. As seen in Table 3, another option to improve statistical errors is to measure the peak line density rather than the beam size. Rather than yielding emittance, this would depend on the phase space density in the core of the beam, which may be as useful for optimizing luminosity.

Future work will focus on coordinating the design of the BDS with the requirements for a laser wire scanner, and on studying the usefulness of the emittance measurement for beam feedback and optimization. The backgrounds may need to be reduced by further collimation or better shielding of the detector. The required laser power is a concern, but is not unreasonable. Because a major difficulty is with poor statistics, more measurements per emittance scan can resolve this difficulty at the expense of a longer measurement time. For the current configuration, with a detector having a time resolution of 3 ns, emittance measurements with an accuracy of better than 10% seem feasible. Because the laser cross-section increases with laser wavelength but grows inversely with beam size, the LWS may paradoxically require beam sizes close to the resolution limit of the laser light in order to work properly. A single, high-accuracy measurement of beam emittance in one plane may require scanning up to 100 pulses, over a period of 1 second.

References

[1] T. Lefevre, "Laser Wire Scanner: Basic Process and Perspectives for the CTFS and CLIC Machines", CLIC Note CERN-OPEN-2002-010, and references therein.

[2] GEANT4 Simulation code reference.

[3] G. Penn, "Simulation of Laserwire in BDS", to be published in *Proceedings of the Nanobeams 2002 Workshop*, CERN, 2003.

[4] J. Bosser, H.H. Braun, E. Bravin et al., "Laser Wire Scanner Development on CTFII", paper TU411 in *Proceedings of the Linac 2002 Conference*, Gyeongju, Korea, 2002.

[5] G. Blair, "Simulation of Laserwire in BDS", to be published in *Proceedings of the Nanobeams 2002 Workshop*, CERN, 2003.